

Comparability in bioactivity assays of 45s5 bioglass scaffolds using simulated body fluid and rabbit blood plasma

Abad-Javier, M.E.¹; Nuñez-Anita, R.E.²; Cajero-Juárez, M.²; Contreras-García, M.E.¹

¹(Advanced Ceramics Department, Instituto de Investigaciones en Metalurgia y Ciencias de los Materiales/Universidad Michoacana de San Nicolás de Hidalgo, México)

²(Proteomic and Cellular Bioengineering Unit, Facultad de Medicina Veterinaria y Zootecnia/ Universidad Michoacana de San Nicolás de Hidalgo, México)

³(Animal Biotechnology Laboratory, Instituto de Investigaciones Agropecuarias y Forestales/ Universidad Michoacana de San Nicolás de Hidalgo, México)³

Abstract :Currently the development of viable biomaterials for replacement of damaged or lost tissue has become a humanitarian need due to the large number of degenerative syndromes and traumas, compromising the tissue and surrounding organs. 45s5 bioactive glass has been exhaustively studied around the world for bone replacement, but it does exist several factors involved in the bioactivity which need to be analyzed, such as local protein presence or differences in carbonate disposition in the surrounding medium. Bioactive scaffolds made of bioglass 45s5 were prepared by the sol-gel via coupled to spray drying, employing polystyrene microspheres as template agents and heat treatment at 700 °C. The bioactivity was examined in vitro with simulated body fluid (SBF) and rabbit blood plasma (RBP), examined by the ability of hydroxyapatite layer to condensate on the material surface. Bioglass scaffolds and hydroxyapatite formation were characterized by X-ray diffraction (XRD), surface electron microscopy (SEM) and energy-dispersive X-ray spectroscopy (EDS). Hydroxyapatite conformation in bioscaffolds incubated in RBP determinate the dependence of CO₂ disposition in order to obtain microspheres conformed by micro whisker, the typically obtained morphology in bioscaffolds incubated in SBF.

Keywords –Bioglass, SBF, rabbit-blood-plasma, bioactivity, hydroxyapatite-morphology

Date of Submission: 14-08-2018

Date of acceptance: 30-08-2018

I. Introduction

Bone reconstitution is a complex process that involves cell process like migration of osteoprogenitor cells engaged to chemical processes like the mineral bone phase degradation and reconstitution, stages responsible of remodeling of the bone. The bone tissue engineering use chemical processes in order to develop active materials to allow the bone formation by their own hydrolysis, these materials also can be structured to contain interconnected pores and higher specifically surface areas bringing on the bioscaffolds production to produce a bone mimetically structure. This bioscaffolds can be used like prosthetic materials and drugs/biomolecules carriers such as growth factors, structural proteins or anti-inflammatory compounds[1].

A fundamental stage in bioscaffolds development for bone regeneration is the formation of a hydroxyapatite layer that serves as a chemical bond between the implant and the organism, this bone-like apatite formation has been studied by in vitro solutions such as SBF and TRIS buffer[2], [3]. Silicate bioactive materials like 45s5 Bioglass release and exchange soluble Si, Ca, P and Na ions, which lead to hydroxyapatite condensation or stimulation at intracellular or extracellular levels[4], although the bonding mechanism bone-scaffold is not well determinate, it is generally believed that hydroxyapatite layer formation is a critical factor for cell adhesion and protein absorption. Simulated body fluid (SBF) has been the most important used test media in the bioactivity analysis, however, although the SBF employs ion concentrations approximately equal to those found on human blood plasma[5], it is difficult to determine what effect the presence of plasma proteins may have on hydroxyapatite condensation, ion absorption on scaffold surface.

Hydroxyapatite, is a calcium phosphate ceramic and act as osteoconductive matrix, allowing bone cells to grow attached, the hydroxyapatite formation rate depends of the Si, Ca and P ions disposition and start with the repolymerization of a SiO₂-rich layer on the surface followed by the migration of Ca²⁺ and PO₄³⁻ groups to the surface forming a hydroxylated CaO-P₂O₅ layer and the consequent crystallization, incorporation of OH⁻, CO₃²⁻ or F⁻ anions from the media form a mixed hydroxyl, carbonate, fluorapatite layer[6]. Additionally, several works employing animal serum or plasma have demonstrated the hydroxyapatite layer condensation inhibition

probably by protein absorption of ions or low carbonate disposition[7], at the same time several researchers determinate the absorption of plasma proteins by the hydroxyapatite layer after 14 days in culture determining the interaction between them[8].

In the present study, we have analyzed the hydroxyapatite layer formation in nanostructured bioglass scaffolds across 2, 4, 6 and 8 days of incubation, in order to determine the morphological and compositional effect occasioned by protein and carbonate ion presence, by the implementation of Rabbit Blood Plasma and SBF prepared by the revised method developed by Oyane and collaborators[5] as comparison control.

II. Materials & Methods

II.I Synthesis. Bioglass powders were prepared by the sol-gel technique coupled to spray drying, bioglass synthesis started from tetraethyl orthosilicate hydrolysis in aqueous solution of nitric acid 0.1 M, adding separately the precursor salts (triethyl phosphate, calcium nitrate, sodium nitrate and silver nitrate) after 60 minutes agitation periods in between each one, the hydrolysis process was made at room in absence of light to avoid oxidation. Bioglass mimetic scaffolds were prepared by adding polystyrene microspheres as template agent, in a 15 mg/100 mL microspheres/precursor-solution ratio, this template was added once the last bioglass precursor was fully hydrolyzed allowing 45 agitation minutes to homogenize the medium.

II.II Spray drying. Prepared precursors-solution were spray dried in a Yamato ADL40 equipment in order to produce nanosized spheres agglomerated in microspheres. The precursors-solution was injected using a single-phase system through a peristaltic pump at 2.45 mL/min flux, this solution was atomized into micro droplets by using pressurized air at 2 bar (2×10^5 Pascals), the atomized particles were evaporated through a hot air stream at 180 °C and collected by vacuum separation by using a cyclone incorporated into the drying equipment. Samples were maintained at room temperature in desiccating conditions.

II.III Scaffolds formation. Bioglass scaffolds or bioscaffolds were prepared using the 45s5 micro aggregated bioglass previously obtained, mixed with polystyrene microspheres as template added in the last stirring stage the precursor solution preparation to ensure the porous structure control. 1x1-centimeter cylinders were fabricated employing 2 ton pressure in a NT-H5 press for 5 minutes, to be heat treated in order to produce the characteristically phases and eliminating the porogen agent, by thermal decomposition, and deriving the porous structure.

II.IV Heat Treatment. Scaffold samples were heat treated by a five-stage process, it started with a heating rate of 3°C/min until reaching 100 °C, this temperature was maintained for 60 minutes followed by another heating rate of 3°C/min reaching a second plateau at 700 °C during 180 minutes, finally scaffolds were cooled at 3 °C/min until room temperature and preserved at 25 °C in desiccating conditions.

II.V Simulated body fluid preparation. Bioactivity assays were carried about by immersion in Simulated Body Fluid (SBF), the SBF solution was prepared by dissolving sodium chloride, sodium hydrogen carbonate, potassium chloride, di-potassium hydrogen phosphate trihydrate, magnesium chloride hexahydrate, calcium chloride, sodium sulfate, Tris-hydroxymethyl aminomethane in distilled water employing HCl to adjust the pH value at 7.4, according to the protocol proposed by Kokubo and Takadama[5], [9], all chemicals employed were reagent grade and stored in a desiccator for 48 hours.

II.VI Rabbit plasma obtention. Rabbit blood samples were collected in EDTA-free containers and stored at 4 °C for 15 minutes, later samples were separated in conical tubes and centrifuged at 12,000 G. Fractions were separated recovering only the supernatant discarding the sediments. The recovered fluid was autoclaved at 15 psi for 10 minutes, repeating the storage and the centrifugation stages two more times recovering the supernatant and keeping it at 4 °C.

II.VII Bioactivity assays. *In vitro* bioactivity of the scaffolds was determined by immersion in simulated body fluid at 37 °C, light free in static position. The scaffolds sample sizes were standardized in 5x5 mm, dried at 100 °C and stored in plastic containers for 24 hours in a desiccator before immersion. The fluid/scaffold ratio was 2mL per gram (for both media, simulated body fluid and rabbit blood plasma) and the fluid was changed every 24 hours, collecting samples every 48 hours for analysis. Collected samples were 5 times washed with deionized water to eliminate fluid remnants and dried at 27 °C for two days after been stored in a desiccator to eliminate the residual humidity.

II.VIII Characterization. Physicochemical characterization was carried out by using an X-Ray Diffraction (XRD), D8 ADVANCE BRUKER DAVINCI equipment with CuK α radiation for phases

determination, measurements were performed before and after heat treatments using a step of 0.4° (2θ), a time per step of 4s and a range from 15 to 8θ . A JEOL JSM-7600F coupled to aEnergy dispersive spectrometry (EDS) detector were employed for morphological and compositional characterization, in order to determine the evolution of the structure across the bioactivity assays lapses.

II.IX Protein quantification. Rabbit plasma proteins were quantified to standardize the concentration in order to maintain this parameter as a repeatability factor, the process was carried out by the Bradford Method, employing Bovine Serum Albumin as standard, Bradford Reactant and 100mM Phosphate Buffer pH 7.0, different concentration standards were adjusted to 25, 50, 75, 100 and 125 mM/mL while the problem sample was diluted at 1:2, 1:5 and 1:10 rates. Bradford reactant was added in each sample and incubated for 2 minutes at 27 °C, then samples absorbance was determined at 595 nm and the calibration curve is constructed determining the correspondent equation by linear regression.

III. Results and Discussion

III.I Bioglass synthesis. Bioglass microspheres added with polystyrene spheres (Fig. 1A) were prepared by using the best synthesis parameters determined in previous works [10], [11], morphology was determined by employing scanning electron microscopy where spherical microaggregates with 15-20 μm nominal diameter were found, simultaneously energy-dispersive x-ray spectroscopy analysis determined the characteristically elemental composition of 45s5 bioglasses (Fig. 1B) and the presence of silver accordingly to the fraction added in the sol-gel preparation (1.75%) [12] with some residual nitrogen coming from the sol-gel precursors hydrolysis. Structural characterization by x-ray diffraction determinate thereactant contamination as nitrate (Fig. 1C), a secondary product in the sol-gel process. Bioglass added with polystyrene spheres maintains the previously reported morphological characteristics as agglomerated microspheres [11].

III.II Bioglass scaffolds characterization. Macrostructure and microstructure analysis of the scaffolds shown highly porous interconnected structure and porosity above 85% (Figure 2A), this well-defined porous structure confere the typical structure of developing bone, obtaining a lower pore structure than scaffolds produced by Gorustovich et. al. [13], who employed the foam replica method, using higher temperature to produce more compact structures with broader pore distribution, they also developed the typical elemental composition of 45s5 bioglass based scaffolds reported by another authors [12]. In this work, the obtained composition is shown in (Figure 2B), demonstrating the template agent allows the obtention of contamination-free scaffolds composition. EDS analysis determined the correct proportion of Si (1.74 keV), Na (1.041 keV), Ca (3.961 keV), Ag (2.984 keV) and P (2.013 keV) in the material composition and the absence of N of the precursor solution and another contaminations, detecting the C (0.277 keV) fraction in noise levels coming from the adhesive used to fix the sample on the sample holder (Figure 2b). DRX study (Figure 2C) revealed the presence of the $\text{Na}_6\text{Ca}_3\text{Si}_6\text{O}_{18}$ (JCPDS #77-2189) and $\text{Na}_2\text{Ca}_4(\text{PO}_4)_2\text{SiO}_4$ (JCPDS# 32-1053) phases [14], [15], demonstrating the correct crystallization process even in the template presence by heat treatment, determining a lower temperature necessary to produce the $\text{Na}_2\text{Ca}_4(\text{PO}_4)_2\text{SiO}_4$ phase, despite another works were necessary to reach temperatures above 850 °C to produce it [16]. Bioglass scaffold diffractogram present curvature in the base line, representative evidence of an amorphous glass fraction in the scaffolds structure. From the X-ray diffractogram the crystalline/amorphous ratio was estimated as 2.35. It's important for bioactive scaffolds conserve this amorphous fraction in order to acquire higher bioactivity resulted of the faster hydrolysis and disposition of Si, Ca and P ions of amorphous, it has been demonstrated by several authors that higher crystallization degree bring to more inert materials [17], [18].

III.III In vitro bioactivity assays by simulated body fluid. Synthesized scaffolds were tested in simulated body fluid as control for 2, 4, 6, & 8 days (Figure 3). The morphological characterization demonstrates hydroxyapatite condensation started at the second incubation day (Figure 3A). The hydroxyapatite formation on the scaffold surface corresponds to the commonly reported morphology classified as cauliflower-like spheres [17], [18]. The $\approx 0.5 \mu\text{m}$ diameter hydroxyapatite clusters started to growth individually and separately from each other before the sixth incubation day, later, when the hydroxyapatite layer covered the entire surface, a process of cluster agglomeration started with the consequent losing of individual clusters.

Elemental composition evolution during the sametime lapse (Figure 4) denotes the silica (1.74 keV) fraction reduction in the scaffold and the increase in phosphorous (2.013 keV), calcium (3.691 keV), oxygen (0.523 keV) and chlorine (2.622 keV) fractions elements, process corresponded to bioglass where the hydrolysis process developed by the aqueous medium lead the liberation of $\text{Si}(\text{OH})_4$ to the environment while the Si-OH groups produced on the bioglass interface attract calcium and phosphate ions from the surrounding media, also previously hydrolyzed ions from the bioglass or coming of the simulated body fluid composition. Also the

incorporation of OH⁻, CO₃²⁻ or Cl⁻ ions from the solution leads the formation of substituted hydroxyapatite, process demonstrated by the increase in the chlorine content, effect reported by other authors who also obtained hydroxyapatite microsphere morphology [19], [20].

III.IV *In vitro* bioactivity assays by rabbit plasma. Obtained rabbit plasma protocol leads the obtention of stable blood plasma with 10 mg/mL protein concentration with a minimal fraction of coagulant factors to ensure the plasma solution stability. As the control bioactivity assays, the analysis of bioglass in rabbit blood plasma incubation times corresponds to 2, 4, 6 and 8 days (Figure 5), similar to the control samples a new phase start to growth by the second incubation day (Figure 5A) but its morphology differs significantly with the control hydroxyapatite layer (Figure 3). This new condensed phase develops a column-like morphology, displaying increasing diameters and elongation among the incubation time, reaching a final 0.1 x 30 μm size. This morphology type is consistent with previously reported hydroxyapatite condensation process, where the lower carbonate content in the medium leads to more elongated column-like morphologies, developing a reaction in which the carbonate ion is displaced by another substitution like OH⁻ or Cl⁻ [21], [22].

Energy-dispersive X-ray spectroscopy analysis (Figure 6) does not determine significant changes in the elemental composition evolution by comparing to control samples except for the chloride peak (2.622 keV), both SBF and rabbit blood plasma incubated scaffolds developed an EDS spectra correspondent to the pure hydroxyapatite control (Figure 6). Similarly as in the simulated body fluid system, the phosphorous (2.013 keV), calcium (3.961 keV) and oxygen (0.523 keV) peaks increase while the silica signal decreases (1.74 keV), indicating a correct hydroxyapatite condensation process, at the same time it could be demonstrated the absence of nitrogen signal (0.392 keV) indicating there is no protein absorption by the material after incubation in rabbit blood plasma, discarding local proteins interference in the scaffold bioactivity, in contrast with several works where protein presence could modify the surface charge and microstructure generating a less bioactive material [23], [24].

III.V Phase determination for bioactivity assays. X-ray diffraction results (Figure 7) confirmed the phosphorous and calcium layer identity as hydroxyapatite (JCPDS #09-0432) and the presence of cristobalite (JCPDS #01-0424), this second produced by the scaffold hydrolysis developing a new silica composed layer [25]. Rabbit blood plasma and simulated body fluid incubated scaffolds (Figure 7) determined at least five hydroxyapatite peaks corresponding to the pure hydroxyapatite control (Figure 7C), determined at 25.861° [0,0,2], 31.773° [2,1,1], 32.151° [1,1,2], 32.9° [3,0,0], and 50.475° [3,2,1] by the eight-incubation day, while two peaks related to cristobalite phase were defined at 21.458° [1,1,1] and 35.463° [2,2,0]. Hydroxyapatite peaks in the simulated body fluid-soaked scaffolds were sharper than rabbit blood plasma-soaked scaffolds, due to a better crystallization probably because of partially chloride substitutions in the hydroxyapatite layer, according to the EDS semi quantitative elemental analysis but not differentiable by XDR due to the similar composition and patterns. In contrast to another work groups the defined pattern of the hydroxyapatite layer shows defined peaks and not only an amorphous layer formation by the 8 eight day [26], demonstrating the improved bioactivity.

III.VI Atmosphere effect in hydroxyapatite morphology. In order to establish the carbonate ion effect on the hydroxyapatite scaffold bioactivity, several samples were incubated for eight days in controlled 3% CO₂ atmosphere at 37 °C once it was soaked in rabbit blood plasma with and without previous 24 hour incubation (Figure 8), in order to recreate the blood vessels environment and the gas availability effect, this treatment develops a morphology correction in the hydroxyapatite layer formation, enhancing the theory of the carbonate ion necessity to develop the cauliflower-like morphology. Bioglass soaked in rabbit blood plasma with the previously 24 h incubation in the 3% CO₂ controlled atmosphere (Figure 8C) develops the typical cauliflower-like configuration while the samples soaked with the untreated rabbit blood plasma (Figure 8B) but incubated in controlled atmosphere present the column-like morphology covered with cauliflower-like hydroxyapatite, this bimodal morphology determine the hydroxyapatite morphological dependence for the carbonate ion presence, enhancing the hypothesis that once carbonate ion is adsorbed by the medium, the morphological development stops the column formation and starts the cauliflower-like phase condensation. Control samples (Figure 8A) incubated at normal atmosphere conditions (approximately 0.4% CO₂) shows the column-like morphology with the same final diameter and elongation displayed in previous experiments (Figure 5D).

Semiquantitative elemental determination by EDS (Figure 9) determine the silica (1.739 keV) fraction diminution and the phosphorous (2.013 keV), calcium (3.690 keV) and chloride (2.621 keV) increase without significant differences between the different treatments, this analysis shows a significant presence of carbonate

in the hydroxyapatite layer, in order to surpass the sample holder noise, confirmed by x-ray diffraction patterns presenting a slight shortening in the a-axis in the samples, except for the samples not soaked in controlled atmosphere, this effect could be determined by the [3,0,0] reflection displaced slightly to the left, produced by carbonate substitution in the hydroxyapatite chemical structure[22].

IV. Conclusion

By the sol-gel synthesis coupled to spray drying with polystyrene spheres template, a hierarchical porous scaffold with high surface reactivity were obtained able to develop a hydroxyapatite homogenous layer by the fourth incubation day with different morphologies depending on the used test media, this scaffold contains the commonly reported crystalline phases and the elemental composition of the 45s5 bioglass. This improved bioactivity was reached by the develop of high surface area by the pore formation and a 2.35 ratio of crystalline/amorphous phase.

The principal difference between SBF and Rabbit Blood Plasma incubation media, is the hydroxyapatite layer morphology, where it was found that rabbit blood plasma developed column-like aggregates, a typical morphology in hydroxyapatite condensation in limited carbon content media, it was proved that in controlled CO₂ atmosphere the adsorbed carbon can turn the hydroxyapatite develop to the cauliflower-type morphology, in early or advanced soaking times. By DRX it was found that SBF medium produce a higher crystallized hydroxyapatite layer than the produced by the rabbit blood plasma, while the EDS analysis didn't show any difference in the composition. Also, it was proved the non-significantly protein presence effect in the bioactivity by EDS analysis where spectra didn't show the characteristic nitrogen content of the amino acids proving the obtention of protein-free hydroxyapatite layer.

Acknowledgements

The authors acknowledge the financial support of CIC-UMSNH and CONACYT. Also acknowledge the IIAF and CMEB-FMVZ, UMSNH for the capacitation and the technical assistance.

References

- [1] S. Bose, M. Roy, and A. Bandyopadhyay, Recent advances in bone tissue engineering scaffolds, *Trends in Biotechnology*, 30(10), 2012, 546–554.
- [2] M. Bohner and J. Lemaître, Can bioactivity be tested in vitro with SBF solution?, *Biomaterials*, 30, 2009, 2175–2179.
- [3] C. Vichery and J.M. Nedelec, Bioactive Glass Nanoparticles: From Synthesis to Materials Design for Biomedical Applications, *Materials*, 9(4), 2016, 288–304.
- [4] L.C. Gerhardt and A. R. Boccaccini, Bioactive Glass and Glass-Ceramic Scaffolds for Bone Tissue Engineering, *Materials (Basel)*, 3(7), 2010, 3867–3910.
- [5] A. Oyane, H.M. Kim, T. Furuya, T. Kokubo, T. Miyazaki, and T. Nakamura, Preparation and assessment of revised simulated body fluids, *J Biomed Mater Res*, 65, 2003, 188–195.
- [6] L.L. Hench, Bioceramics: From Concept to Clinic, *Journal of the American Ceramic Society*, 74(7), 1991, 1487–1510.
- [7] N. C. Blumenthal, F. Betts, and A.S. Posner, Effect of carbonate and biological macromolecules on formation and properties of hydroxyapatite, *Calcified Tissue Research*, 18(1), 1975, 81–90.
- [8] A. El-Ghannam, P. Ducheyne, and I.M. Shapiro, Porous bioactive glass and hydroxyapatite ceramic affect bone cell function in vitro along different time lines, *Journal of Biomedical Materials Research*, 36(2), 1997, 167–180.
- [9] T. Kokubo and H. Takadama, How useful is SBF in predicting in vivo bone bioactivity?, *Biomaterials*, 27(15), 2006, 2907–2915.
- [10] A. Zocca, H. Elsayed, E. Bernardo, C. M. Gomes, C. Knabe, P. Colombo, and J. Günster, 3D-printed silicate porous bioceramics using a non-sacrificial preceramic polymer binder, *Biofabrication*, 7(2), 2015, 1–13.
- [11] M. Abad-Javier, M. Cajero-Juárez, and M. E. Contreras García, 45S5 Bioglass porous scaffolds: structure, composition and bioactivity characterization, *Journal of Silicate Based and Composite Materials*, 68(4), 2016, 124–128.
- [12] G.E. Vargas, R.V. Mesones, O. Bretcanu, J.M.P. López, A.R. Boccaccini, and A. Gorustovich, Biocompatibility and bone mineralization potential of 45S5 Bioglass®-derived glass-ceramic scaffolds in chick embryos, *Acta Biomaterialia*, 5(1), 2009, 374–380.
- [13] A.A. Gorustovich, G.E. Vargas, O. Bretcanu, R. Vera Mesones, J.M. Porto López, and A.R. Boccaccini, Novel bioassay to evaluate biocompatibility of bioactive glass scaffolds for tissue engineering, *Advances in Appl. Ceramics*, 107(5), 2008, 274–276.
- [14] F.M. Stáble and C. Volzone, Bioactivity of leucite containing glass-ceramics using natural raw materials, *Journal of Materials Research*, 17(4), 2014, 1031–1038.
- [15] D. Bellucci, A. Sola, and V. Cannillo, A Revised Replication Method for Bioceramic Scaffolds, *Bioceramics Development and Applications*, 1, 2011, 1–8.
- [16] L. Lefebvre, L. Gremillard, J. Chevalier, R. Zenati, and D. Bernache-Assolant, Sintering behaviour of 45S5 bioactive glass, *Acta Biomaterialia*, 4(6), 2008, 1894–1903.
- [17] G.M. Luz and J.F. Mano, Preparation and characterization of bioactive glass nanoparticles prepared by sol-gel for biomedical applications, *Nanotechnology*, 22(49), 2011, 1–11.
- [18] Z. Hong, R.L. Reis, and J.F. Mano, Preparation and in vitro characterization of novel bioactive glass ceramic nanoparticles, *Journal of Biomedical Materials Research*, 88(2), 2009, 304–313.
- [19] J. Zhong and D.C. Greenspan, Processing and properties of sol-gel bioactive glasses, *Journal of Biomedical Materials Research*, 53(6), 2000, 694–701.
- [20] G. Kirste, J. Brandt-Slowik, C. Bocker, M. Steinert, R. Geiss, and D.S. Brauer, Effect of chloride ions in Tris buffer solution on bioactive glass apatite mineralization, *International Journal of Applied Glass Science*, 8(4), 2017, 438–449.
- [21] H. Pan and B.W. Darvell, Effect of Carbonate on Hydroxyapatite Solubility, *Crystal Growth & Design*, 10(3), 2010, 3–8, 2010.
- [22] R.Z. Legeros, O.R. Trautz, J.P. Legeros, E. Klein, and W.P. Shirra, Apatite crystallites: effects of carbonate on morphology.,

Comparability in bioactivity assays of 45s5 bioglass scaffolds using simulated body fluid and

- Science*, 155(3768), 1967, 1409–1411.
- [23] H.H. Lu, S.R. Pollack and P. Ducheyne, 45S5 Bioactive glass surface charge variations and the formation of a surface calcium phosphate layer in a solution containing fibronectin, *Journal of Biomedical Materials Research*, 54(3), 2000, 454-61.
- [24] A. El-ghannam, E. Hamazawy, and A. Yehia, Effect of thermal treatment on bioactive glass microstructure, corrosion behavior, zeta potential, and protein adsorption, *Journal of Biomedical Materials Research*, 55(3), 2000, 387-395.
- [25] P. Siriphannon, Y. Kameshima, and A. Yasumori, Formation of hydroxyapatite on CaSiO₃ powders in simulated body fluid, *Journal of the European Ceramic Society*, 22, 2002, 511–520.
- [26] N. Shankwar and A. Srinivasan, Evaluation of sol-gel based magnetic 45S5 bioglass and bioglass-ceramics containing iron oxide, *Materials Science and Engineering: C*, 62, 2016, 190–196.

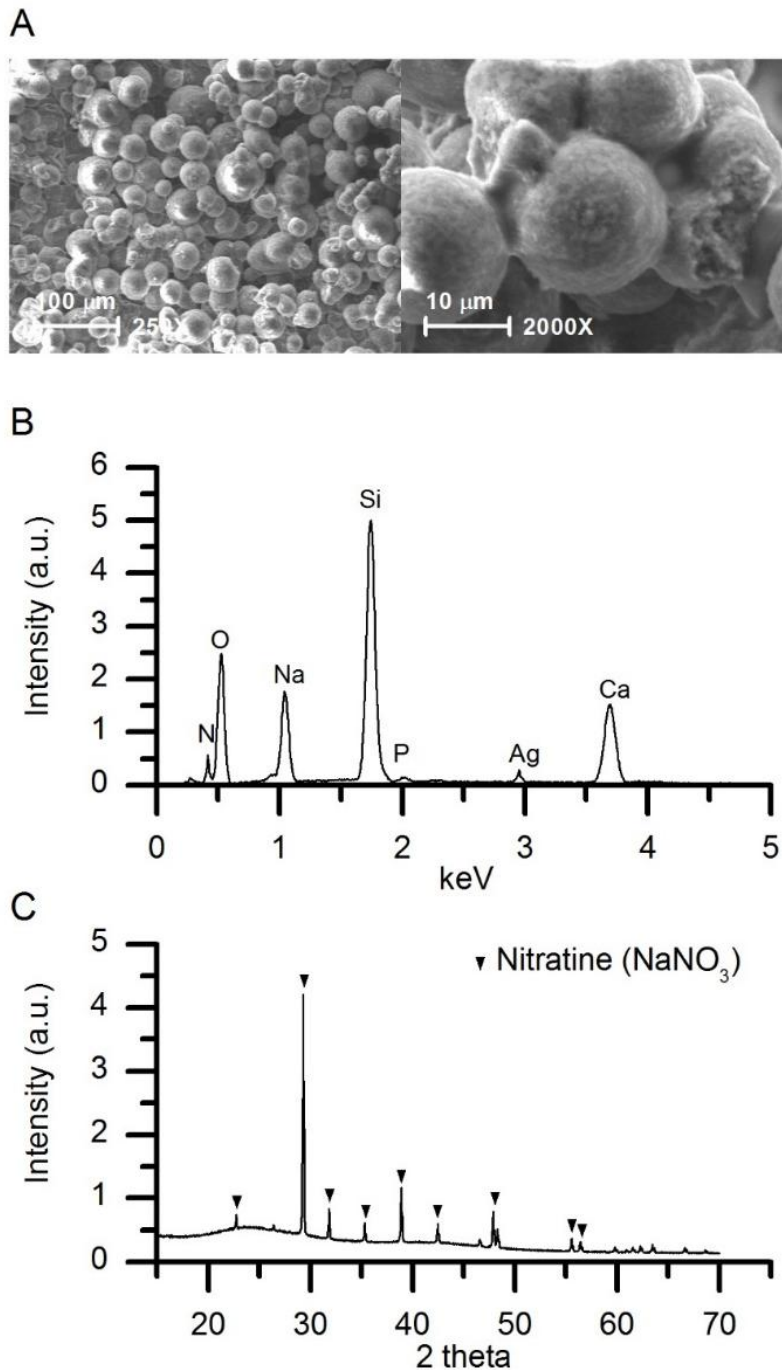


Figure 1. Scanning electron micrographs (A), energy-dispersive X-ray analysis (B) and X-ray diffraction pattern (C) of Bioglass 45s5 spherical microagregates added with polystyrene microspheres as template agent before spray drying treatment.

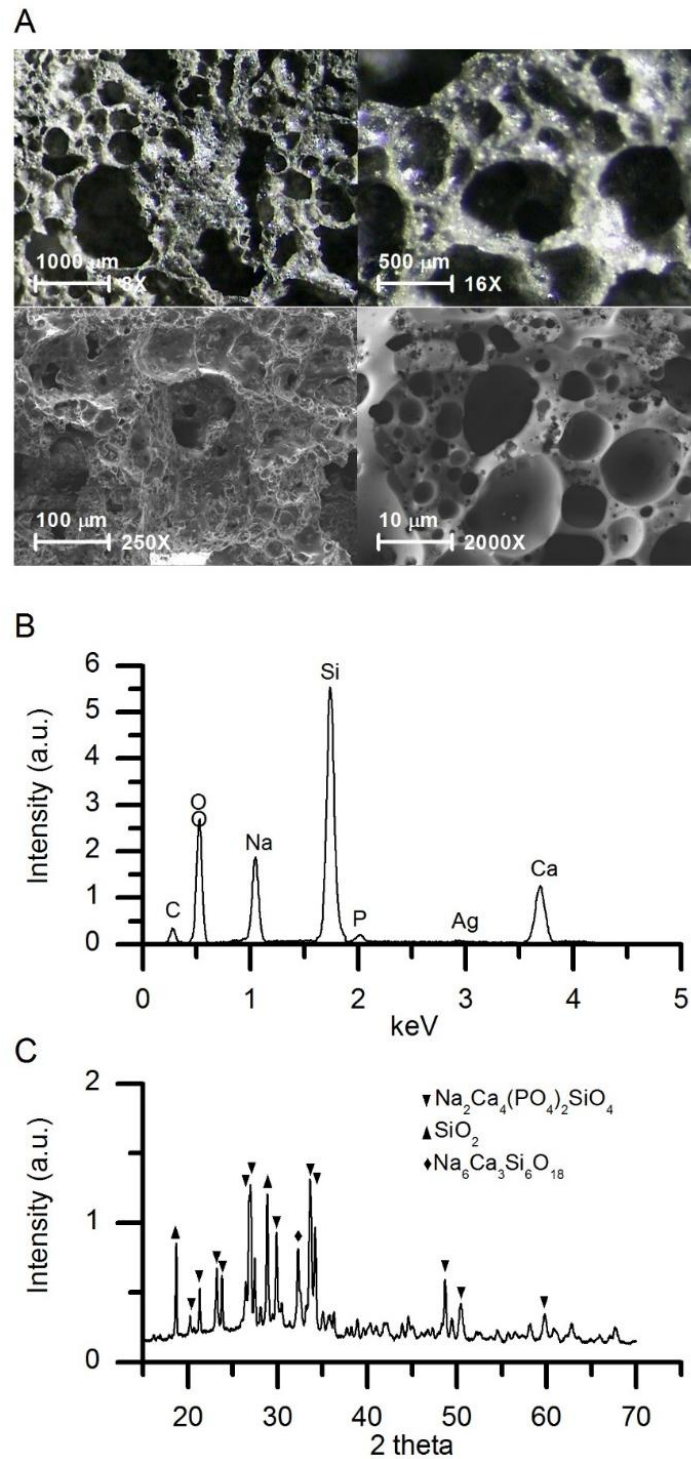


Figure 2. Scanning electron micrographs (A), energy-dispersive X-ray analysis (B) and X-ray diffraction pattern (C) of Bioglass 45s5 bioactive scaffold (bioscaffolds) after heat treatment at 700 °C for 3 hours.

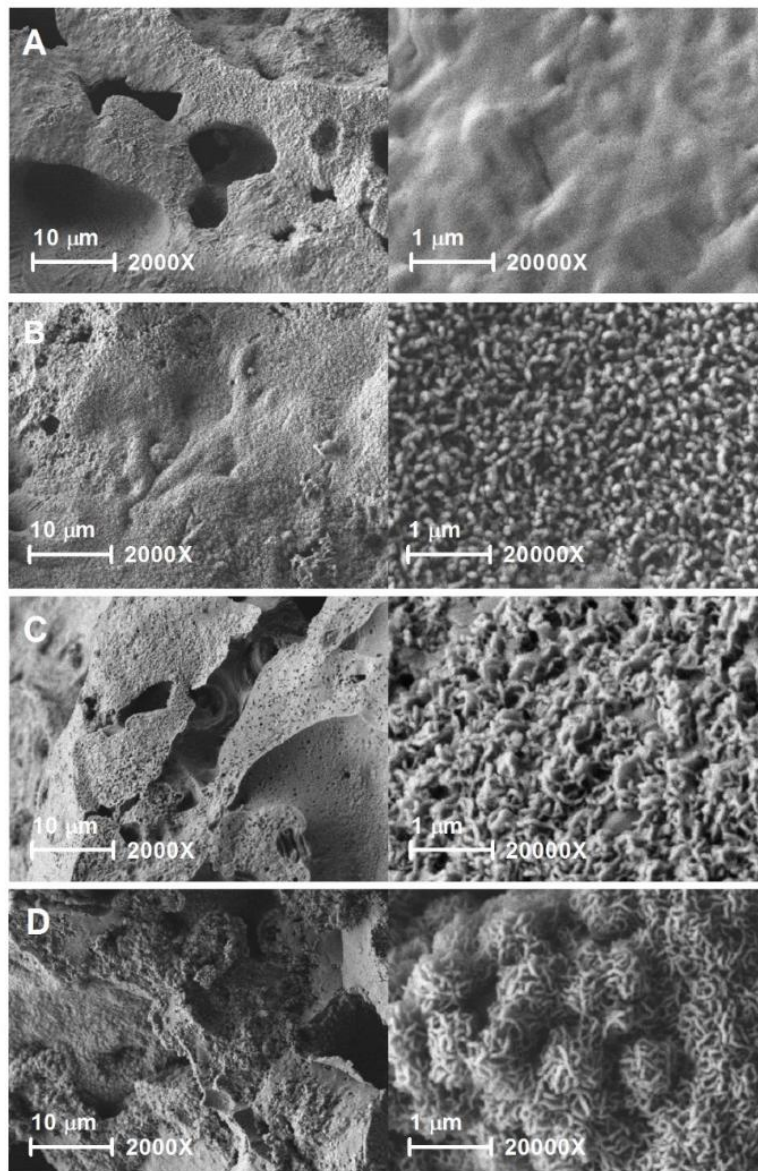


Figure 3. Scanning electron micrographs of bioglass scaffolds immersed in simulated body fluid after 2 (A), 4 (B), 6 (C) & 8 (D) days, revealing cauliflower-like apatite clusters after four incubation days.

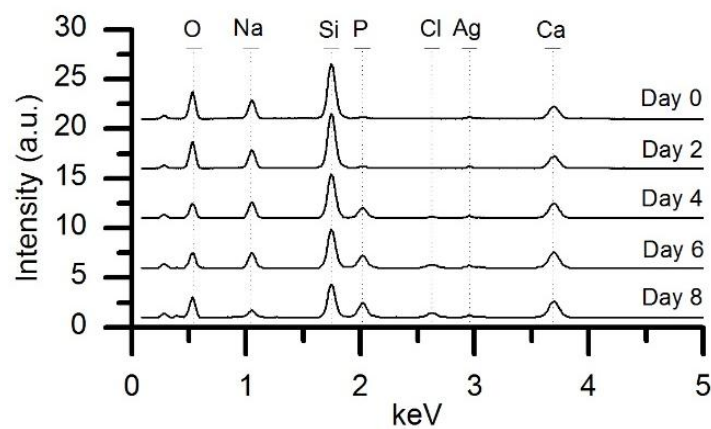


Figure 4. Energy-dispersive X-ray semi-quantitative analysis of bioglass scaffolds immersed in simulated body fluid after 0, 2, 4, 6 & 8 days.

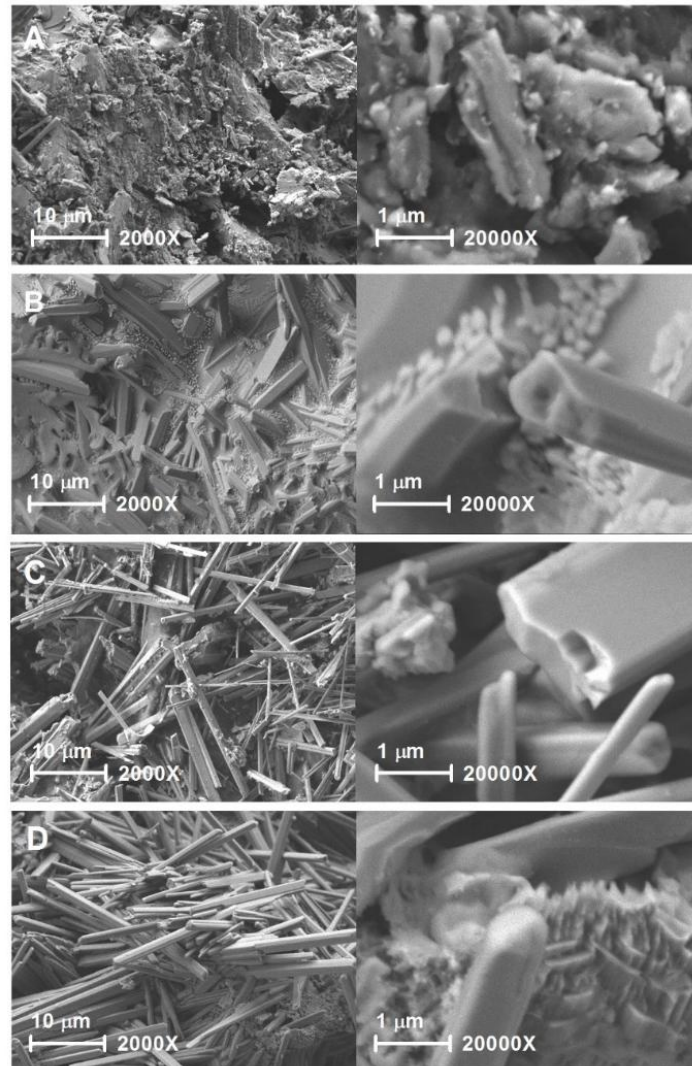


Figure 5. Scanning electron micrographs of bioglass scaffolds immersed in rabbit blood plasma after 2 (A), 4 (B), 6 (C) & 8 (D) days, revealing needle-like apatite constructions after four incubation days.

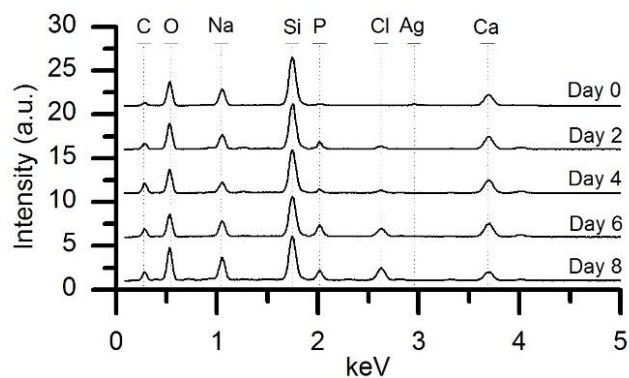


Figure 6. Energy-dispersive X-ray semi-quantitative analysis of bioglass scaffolds immersed in rabbit blood plasma after 0, 2, 4, 6 & 8 days.

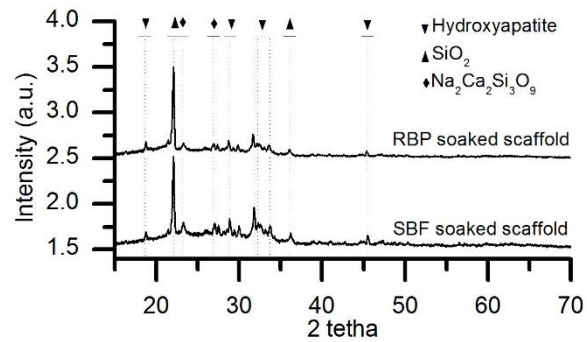


Figure 7. X-ray diffraction patterns of bioglass scaffolds after been soaked in simulated body fluid (SBF) and rabbit blood plasma (RBP) for 8 days.

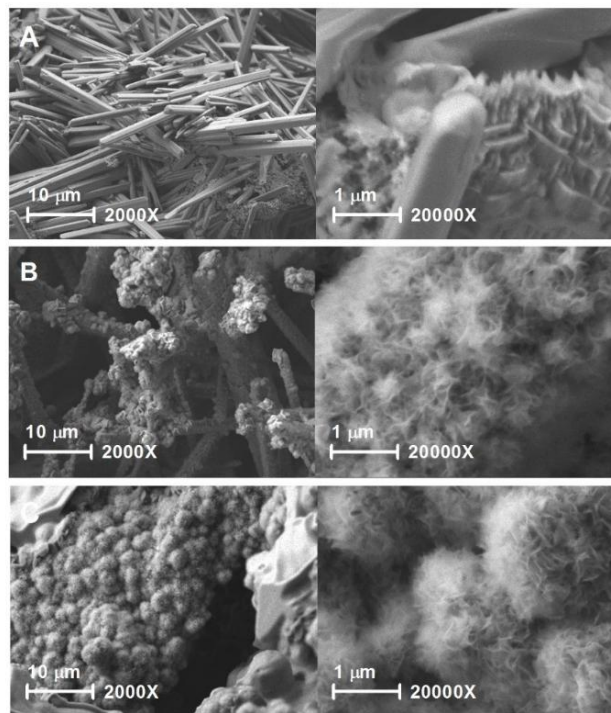


Figure 8. Scanning electron micrographs of bioglass scaffolds immersed in rabbit blood plasma for 8 days in normal atmosphere (A), 5% CO₂ controlled atmosphere (B) and 24 hours previously incubated rabbit blood plasma in 5% CO₂ controlled atmosphere (C).

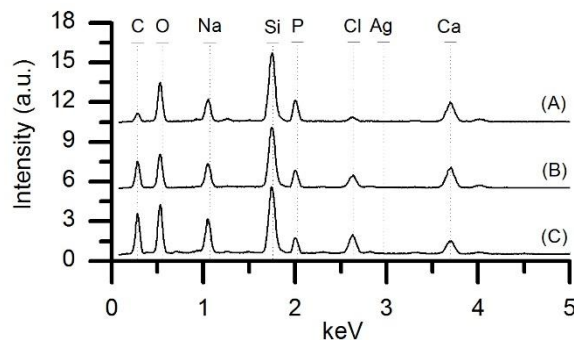


Figure 9. Energy-dispersive X-ray semiquantitative analysis of bioglass scaffolds immersed in rabbit blood plasma for 8 days in normal atmosphere (A), 5% CO₂ controlled atmosphere (B) and 24 hours previously incubated rabbit blood plasma in 5% CO₂ controlled atmosphere (C).

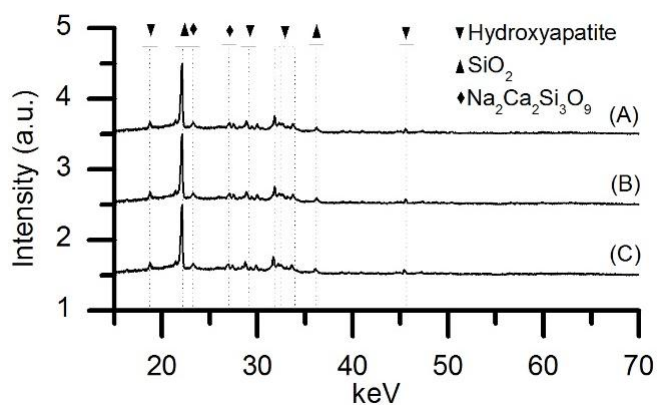


Figure 10. X-ray diffraction patterns of bioglass scaffolds immersed in rabbit blood plasma for 8 days incubated in normal atmosphere (A), 5% CO₂ controlled atmosphere (B) and 24 hours previously incubated rabbit blood plasma in 5% CO₂ controlled atmosphere (C).

Abad-Javier " Comparability in bioactivity assays of 45s5 bioglass scaffolds using simulated body fluid and rabbit blood plasma ." IOSR Journal of Pharmacy and Biological Sciences (IOSR-JPBS) 13.4 (2018): 13-23